Journal of the European Ceramic Society **18** (1998) 653–659

PII: S0955-2219(97)00172-6
0955-2219/98/$19.00 + 0.00

Characterisation of an Oxidation Layer on Reaction Bonded Mullite/Zirconia Composites by Indentation

X. Miao,[a] S. Scheppokat,[b] N. Claussen[b] and M. V. Swain[a]*

[a]CSIRO Division of Applied Physics, Lindfield, New South Wales, 2070, Australia
[b]Advanced Ceramics Group, Technische Universitat Hamburg-Harburg, 21071 Hamburg, Germany

(Received 18 April 1997; accepted 26 September 1997)

Abstract

An oxidised outer layer that was formed on reaction bonded mullite/zirconia composites and the difference in the mechanical properties between this layer and the bulk material were investigated using an ultra micro indentation system (UMIS) combined with XRD and high resolution SEM. It was shown that the bulk consisted of mullite and tetragonal zirconia as well as some residual alumina and SiC. The outer layer consisted of mullite and larger grain-sized zirconia as well as a small amount of zircon. About 60% of the zirconia was transformed from tetragonal to monoclinic phase in the layer. It was found that the bulk had higher hardness but lower toughness than the outer layer. Indentation testing revealed the presence of residual compressive stress in the outer layer, which was attributed to the different degrees of t- *to* m-ZrO_2 *transformation, different fractions of mullite, and different coefficients of thermal expansion in the layer versus the bulk.* © *1998 Elsevier Science Limited. All rights reserved*

1 Introduction

Mullite ceramics have excellent thermomechanical properties with potential for high-temperature applications.[1] However the mechanical properties, especially strength and toughness, of pure mullite ceramics at low temperatures are not outstanding. Significant improvements have been achieved by incorporating high strength, high modulus second phase ceramic reinforcements.[2] Sol–gel processing and hot pressing are normally used to prepare these composites. However, simple and more cost-effective processes are still in demand to compete favourably with the available production methods.

A process for producing reaction bonded alumina based ceramics (abbreviated to RBAO process) has been developed[3–7] at the TUHH, which is technologically simple, involving traditional fabrication steps, i.e. attrition milling of Al and Al_2O_3 containing mixtures, forming by methods as used in normal powder metallurgy, and heat treatment in air to oxidise the Al into Al_2O_3. High-strength alumina-based ceramics with a wide range of compositions and microstructures can be produced using the RBAO process. This process has been modified to produce mullite based ceramics and is accordingly named as the reaction bonding process for mullite based ceramics (abbreviated to RBM process).[6,7] This process provides additional net-shape forming potential due to the associated volume expansion during reaction compensating for the sintering shrinkage.

Mullite/zirconia composites have been prepared in the TUHH by the RBM process. A novel feature of these RBM materials is the presence of a white outer layer on the grey bulk material after sintering. This layer is about 0·4 mm thick after sintering at standard conditions (1·5 h at 1550°C). While previous studies have concentrated on the properties of the grey bulk material,[6,7] the aim of the present paper is to evaluate the mechanical properties of the thin outer layer and the inner core using indentation methods. Traditional techniques such as the double cantilever beam (DCB) and the single edge notch beam (SENB) methods involve extensive sample preparation and are suitable for bulk materials only.[8] Indentation methods have advantages over traditional techniques and require only a polished plane surface that is readily attained. Additionally, many indents can be made in a relative small area and locally determine the hardness and the elastic modulus of the material.

*To whom correspondence should be addressed.

With the newly developed nanoindentation technique, hardness and elastic modulus of individual fine-sized grains and phases in composites can be determined.

2 Experimental Procedures

The mullite/zirconia samples used in this study were produced by the RBM process. Powder mixtures containing 24 vol% SiC, 55 vol% Al, 16 vol% ZrO_2 and 5 vol% Al_2O_3 were attrition milled for 5 h at 700 rpm in acetone with TZP milling balls. The powders were dried and sieved, and green compacts were made by uniaxial pressing at 50 MPa and subsequent isostatic pressing at 400 MPa. Both disc- and bar-shaped samples were prepared for this study. The samples were fired according to the following heating cycle: 1° min^{-1} →410°C, 2 h hold, 0·5° min^{-1}→680°C, 2 h hold, 1° min^{-1}→1100°C, 2 h hold, 1° min^{-1}→1150°C, 15 h hold, 10° min^{-1} →1550°C, 1·5 h hold, 10° min^{-1}→RT.

The hold at 410°C was for the removal of a binder used in the forming step. The oxidation of Al started at 680°C and was normally completed at ~800°C. The hold at 1100°C and 1150°C was to oxidise the SiC. To obtain a thicker layer (1 mm), an additional hold for 15 h at 1350°C was included in the heating cycle after the oxidation hold at 1150°C. The materials were sintered to >95% theoretical density at 1550°C. A commercial 3Y-TZP ceramic with grain size of ~0·3 μm was used as a reference for the micro- and nano-indentation experiments.

Samples for indentation testing were cut from the parent composite materials. The outside surface of the outer layer and the cross section containing the white outer layer and the grey inner core were polished down to 1 μm diamond paste. Indentation testing was carried out on a macrohardness testing machine (Vickers-Armstrongs) and a microhardness machine (Zwick & Co. KG.). Loads from 50 to 400 N were used to indent the cross sectional inner core, the cross-sectional outer layer and the outside surface of the outer layer. Figure 1 is a schematic illustration of the location of the various indentation tests on the sample. Indentation testing was also carried out on an Ultra Micro Indentation System (UMIS 2000). In this case, the indents were produced at 200 mN along a line through the outer and core layers at 40 μm intervals. Indentation at load 30 mN with indent interval of 15 μm was also carried out in some selected areas from the inner core and the outer layer. The 3Y-TZP sample was of uniform microstructure and thus all the indentation tests were conducted on an arbitrarily selected polished surface using the same loads as those for the RBM samples.

The dimensional measurement of indents and crack lengths was conducted on a modern optical microscope (Nikon) with XY stage optical encoded scale, high magnification NIC objectives, a video camera and a TV screen. The resultant magnification was as high as 1800×. To improve the reflection of the polished surface, a thin gold film was coated before indentation on the micro and macro hardness testing machines.

Vickers' hardness values were calculated with the standard equation:

$$Hv = 1{\cdot}8544P/(2a)^2$$

where P is the indentation load (kg) and 2a the indentation diagonal (mm). The toughness was calculated based on a half-penny crack configuration and the constant value of $P/c^{3/2}$ for a given material, using the following expression:[9]

$$K_{1c} = 0{\cdot}016(E/H)^{1/2}P/c^{3/2}$$

where E is Young's modulus (GPa); H is hardness (GPa); P is the indentation load (N); c is the crack length (m) from the centre of the pyramid impression to the crack tip.

In the ultra micro indentation system, the hardness and the modulus were determined by the computer software based on the measured penetration depth as a function of indentation load.[10,11] The ultra micro indentation system was fitted with an optical objective-video camera-TV screen system, which was mainly used for the positioning of the indentation at certain points or phases.

High-resolution scanning electron microscope (JEOL JSM 6400 F) was used to analyse the microstructure of samples, to find the location of ultra micro indentation impressions and to study the interaction of the indentation cracks with the materials. Samples were also coated with thin carbon film for SEM observation. Acceleration voltages of 5–25 kV were used for different purposes. Carbon coating before indentation followed by SEM observation had another advantage; the cracks and the impressions were clearly visible due to the localised charging effect, where the coating had cracked during testing. XRD analysis of the white surface and core of samples was also carried out.

3 Results and Discussion

3.1 Microstructure

SEM showed that the white outer layer exhibited higher porosity than the grey inner core (Fig. 2).

Both the outer layer and the inner core contained about 15 vol% of zirconia (appearing white in the SEM micrograph). However, SEM at higher magnification showed that the grain size of the zirconia phases in the outer layer was larger than in the inner core (Fig. 3). X-ray diffraction (XRD) (Fig. 4) showed that the outer layer consisted of mullite, zirconia and a small amount of zircon. About 60 vol% of the zirconia was transformed from the original tetragonal to the monoclinic phase within the outer layer. The inner core consisted of mullite, zirconia and small amounts of alumina and SiC. Essentially all the zirconia in the core was tetragonal.

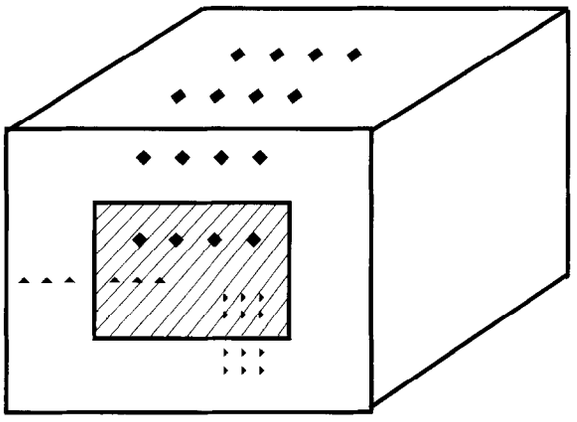

Fig. 1. Schematic diagram showing the locations of the various indentation tests on the mullite-zirconia composite featured with an outer layer and an inner core.

Following these results, the formation of the white layer on the samples can be explained by the oxidation of the residual SiC in the outer zone of the material during sintering. It is assumed that even at a stage when the sample was already densified, oxygen was still able to diffuse into the material and oxidise the residual SiC. The oxidation products of SiC (CO/ SiO) were trapped in the material and this resulted in the porosity in the outer layer.[12,13]

3.2 Macroindentation

Figure 5 shows the plot of crack length c in the form of $c^{3/2}$ as a function of indentation load (P) for the bulk and the outer layer as well as the reference material 3Y-TZP. The data followed a

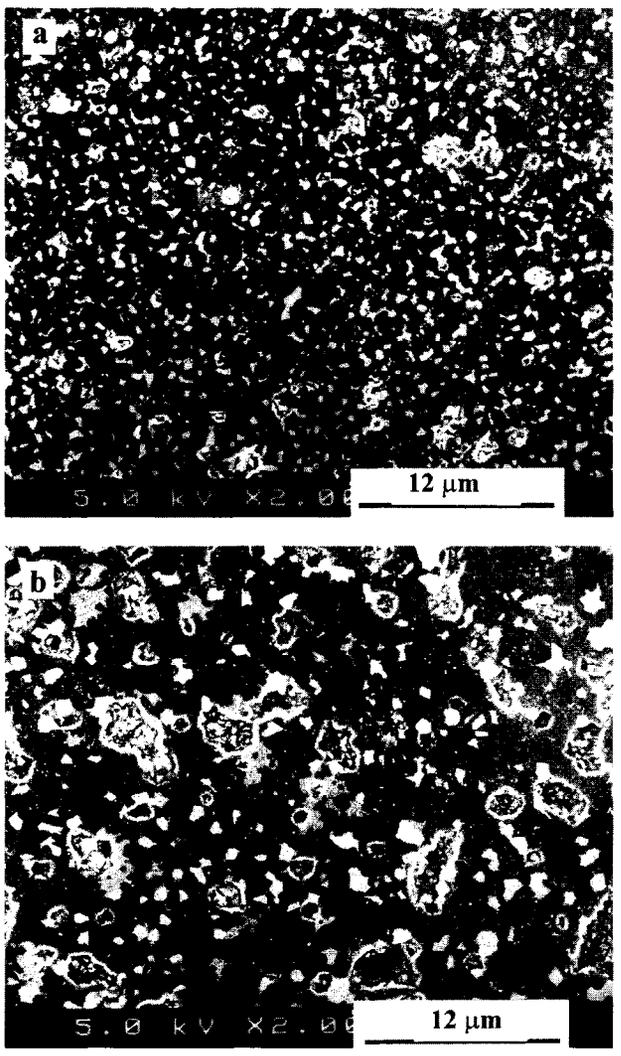

Fig. 2. SEM micrographs showing (a) the dense inner core and (b) the porous outer layer.

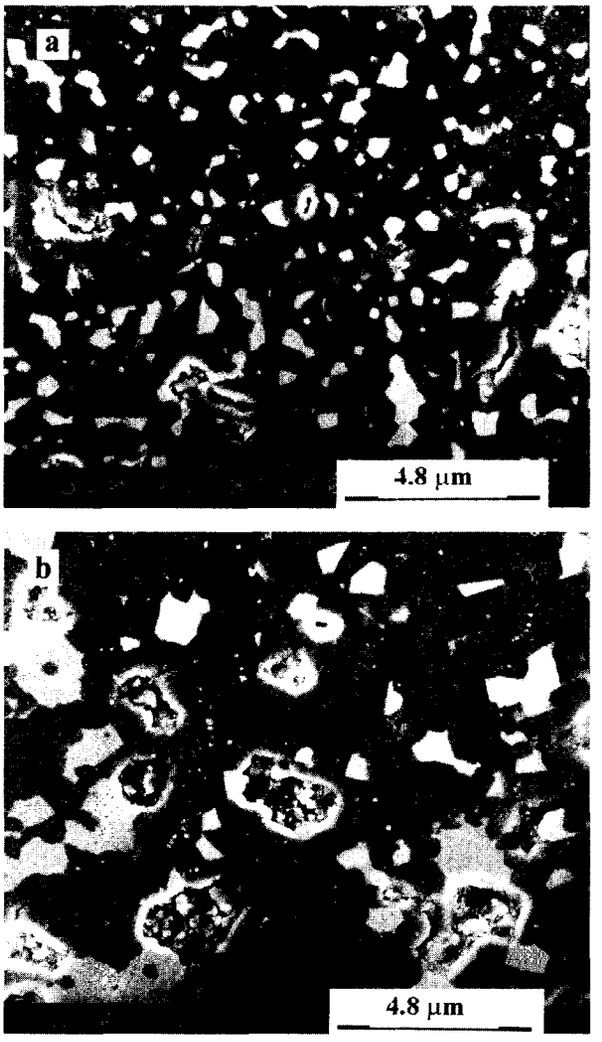

Fig. 3. SEM micrographs showing that the grain size of the white zirconia phases in (a) the inner core is smaller than in (b) the outer layer.

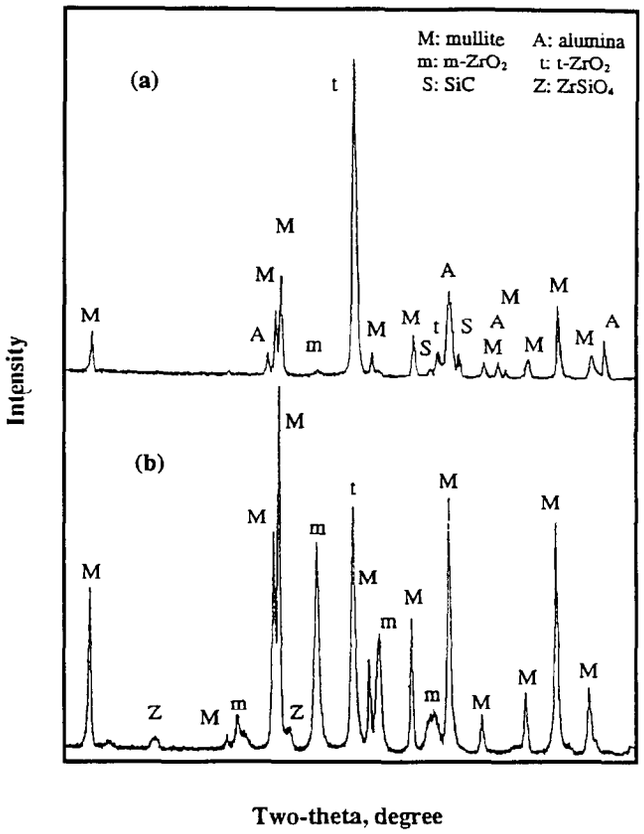

Fig. 4. XRD diagrams showing the different phases present in (a) the inner core and in (b) the outer layer.

linear relationship, that is $c^{3/2}/P$ being a constant, depending on the material. The toughness values were calculated and are shown in Table 1 along with hardness values.

It can be seen that the layer was tougher than the core. The hardness of the inner core was about 2× the hardness of the outer layer. In addition, the toughness and hardness values measured on the cross-section of the white layer were different from the ones measured on the outside surface; lower toughness and hardness values were measured on the cross section of the layer.

This difference in mechanical properties of the inner core and the outer layer can be attributed to the different microstructures of the inner core and the outer layer. The residual SiC and Al_2O_3 in the core made the core harder. The small sized t-ZrO_2 particles in the core were too stable, thus they could not contribute to toughening. The outer layer was less hard because of the higher porosity and the lower inherent hardness of the phases. The higher toughness of the outer layer was due to the more transformable t-ZrO_2 phase and to the fact that the micro-pores also had the effect of stopping cracks from propagating.

The crack patterns in the inner core area had a normal symmetry as were those generated on the outer surface of the layer. However, the crack

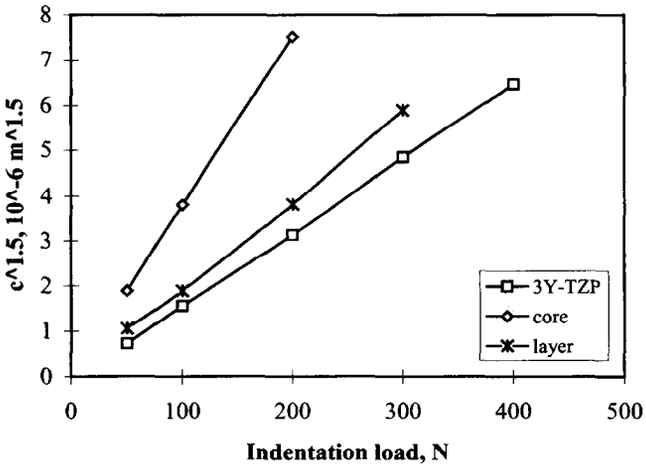

Fig. 5. Plots of $c^{3/2}$ versus load data generated with the Vickers' indenters.

Table 1. Results of the macroindentation

Materials/areas tested	K_{Ic}, *MPa.* $m^{1/2}$	$Hv_{10\,kgs}$
Core/cross section	2·1 ± 0·2	980 ± 26
Layer/cross section	2·9 ± 0·2	389 ± 9
Layer/outside surface	3·7 ± 0·2	425 ± 12
3Y-TZP/polished surface	4·9 ± 0·2	1250 ± 11

patterns from the cross-section of the outer layer and the area in the core close to the boundary between the core and the layer showed a pair of long cracks and a pair of short cracks, with the long cracks parallel to the interface between the core and the outer layer (Fig. 6). This suggests that a residual compressive stress was present in that area. A consequence of the residual compressive stress in the surface region of the sample would be that this stress would contribute to an increase in strength and a reduction in the crack lengths about a Vickers impression and thereby a higher effective toughness.

There are three possible sources for the observed residual compressive stress. First, there was more

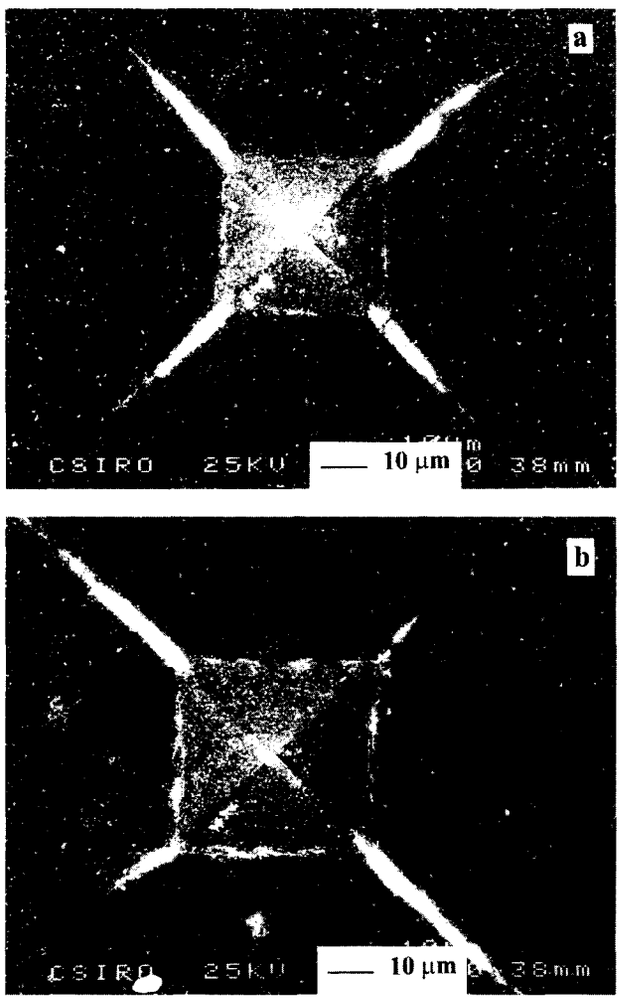

Fig. 6. SEM micrographs showing the normal symmetry of the crack patterns generated with the Vickers' indenter in (a) the inner core and a pair of long cracks perpendicular to a pair of short cracks in (b) the cross-sectional outer layer.

mullite in the outer layer and the mullite formation was accompanied by a volume expansion. Second, the well-known *t*- to *m*-ZrO_2 transformation preferentially in the outer layer because of the larger grain size was again accompanied by a volume expansion. Third, since the outer layer had a different phase composition from the inner core, the mismatch of the thermal expansion coefficients (α) would also lead to residual stress. The core contained some residual SiC and alumina, and a mixture of these two components had a higher α than mullite, resulting in compressive stress in the outer layer after cooling.

The residual compressive stress present in the outer layer may initiate the formation of the trace amount of zircon phase detectable by XRD, i.e.

$$3Al_2O_3 \cdot 2SiO_2 + 2ZrO_2 \Longleftrightarrow 2ZrSiO_4 + 3Al_2O_3$$

A small amount of alumina may coexist although it was not detected by XRD. The density of the alumina (Al_2O_3) and zircon ($ZrSiO_4$) mixture is considerably higher than that of the mullite ($Al_2O_3 \cdot 2SiO_2$) and zirconia (ZrO_2) mixture. In other words, the reaction between mullite and zirconia to form zircon and alumina is accompanied by a volume shrinkage. Therefore, the residual compressive stress favours the formation of the zircon phase.

3.3 Microindentation

Analysis of the microindentation force-displacement data enabled the hardness (equivalent to Vickers' hardness)[14] and the modulus [$E/(1-\nu^2)$, E =Young's modulus, ν =Poisson's ratio] distribution from the inner core through the boundary to the outer white layer to be determined, Fig. 7. The impression area covered both the mullite and the zirconia phases, thus the properties were attributed to the composite material. From Fig. 7, it can be seen that the hardness in the bulk was higher than the outer layer, which was also reflected on the macrohardness testing. The results for the elastic modulus indicate a significant reduction from ~200 ± 10 GPa to 130 ± 15 GPa for the core and the outer regions respectively.

Figure 8 shows the results of the ultra micro indentation tests (UMIS 2000) at the load of 30 mN. In this case, the edge lengths of the indentation impressions were about 1 to 2 μm, similar to the phase size, thus the properties of the individual phase were able to be detected. In Fig. 8, the hardness and the modulus were evenly distributed for the 3Y-TZP. This was because the 3Y-TZP was dense and consisted of fine (~0·3 μm) and homogeneously distributed polycrystals. For the outer

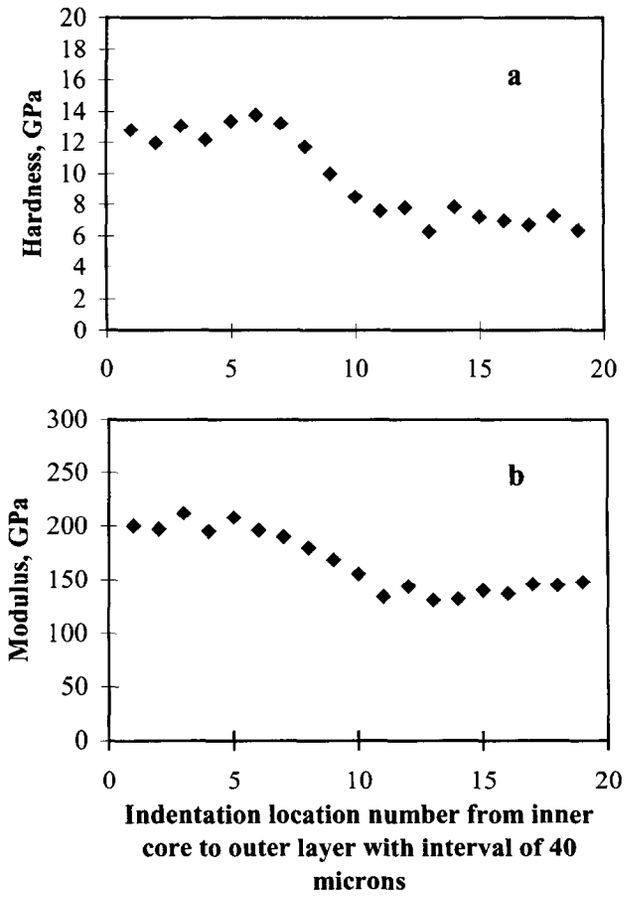

Fig. 7. (a) The hardness and (b) the modulus distribution from the inner core through the boundary to the outer layer (indentation load: 200 mN).

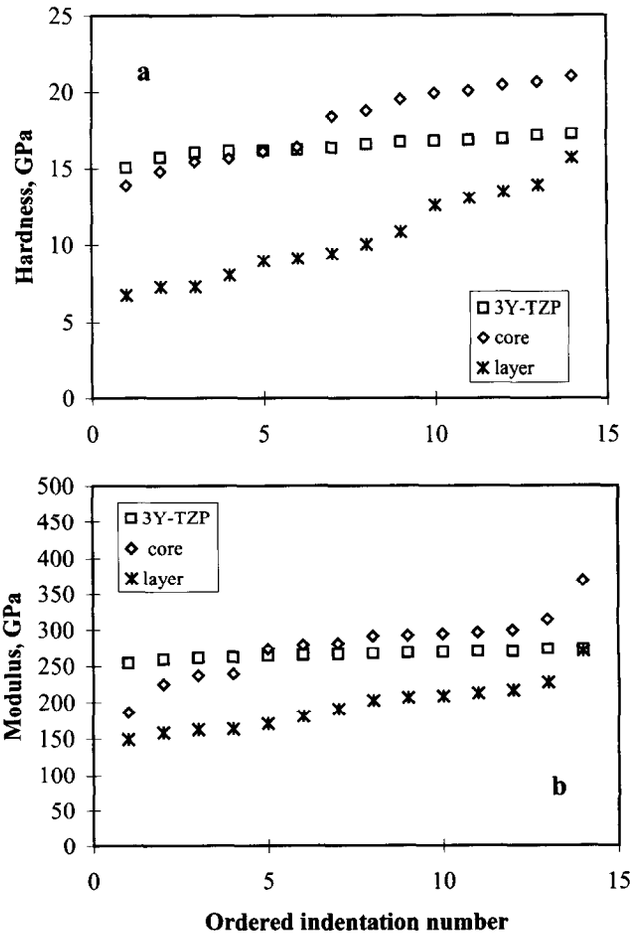

Fig. 8. Results of the ultra micro indentation tests at the load of 30 mN showing (a) the variation of the hardness and (b) the modulus measured at different locations for the inner core and the outer layer in comparison with the 3Y-TZP.

layer of the mullite/zirconia sample, the lowest hardness and modulus values were close to or equal to the porous mullite, whereas the highest values were close to or equal to the zirconia phases. For the inner core, the highest values were close to or equal to the alumina or SiC, whereas the lowest values were close to or equal to the mullite grains, which often contained very fine residual alumina and SiC particles. The assignment of the mechanical properties to the individual phases was confirmed by the SEM observation.

Figures 7 and 8 indicate that the measured hardness depends on the indent size relative to the phases present. If the indent size is much larger than the phase size, the measured hardness is the hardness of the composite. If the indent size is much smaller than the phase size, the measured hardness would correspond to the individual phase, which is less affected by the other surrounding phases. In fact, the elastic modulus of composites can be calculated from volume fraction of different phases determined by XRD according to the rule of mixture. Thus from the values shown in Fig. 8 and the known volume fractions of the specific phases, the composite elastic modulus may be estimated ($E_{comp} = \sum V_{fi}E_i$, where V_{fi} is the volume fraction of the individual phases of elastic modulus E_i):

$$E_{core} = 0{\cdot}16 \times 200(\text{zirconia}) + 0{\cdot}1 \times 360(\text{alumina}) + 0{\cdot}1 \times 400(\text{SiC}) + 0{\cdot}64 \times 144(\text{mullite}) = 200\ \text{GPa}$$

$$E_{layer} = 0{\cdot}16 \times 200(\text{zirconia}) + 0{\cdot}74 \times 144(\text{mullite}) = 138{\cdot}6\ \text{GPa}$$

without taking into account the residual porosity. The calculated elastic modulus of the core and the layer are quite comparable to the measured values shown in the Fig. 7.

4 Conclusions

Indentation testing has demonstrated a significant difference in the hardness, modulus and toughness of the oxidised outer layer from that of the core region of the mullite/zirconia composite. The inner core had a higher hardness (Hv 980 versus Hv 400),

higher modulus (200 GPa versus 140 GPa) but lower toughness (2·1 $MPam^{0·5}$ versus 3·3 $MPam^{0·5}$) than the outer layer.

The zirconia phase of the outer layer was primarily monoclinic whereas that of the inner core was essentially tetragonal. There were other minor changes in composition of the outer layer compared with the inner core, associated with the complete oxidation of SiC to form mullite. The microstructure of the outer layer was higher in porosity and the grain size of the zirconia phase was coarser than in the core region. The inner core consisted of ~64 vol% mullite, ~16 vol% zirconia, ~10 vol% alumina, and ~10 vol% SiC. The outer layer consisted of ~74 vol% mullite, ~16 vol% zirconia, and ~10 vol% pores.

Cracking from indentation tests indicated that a compressive stress existed within the outer zone which was possibly associated with the high amount of monoclinic zirconia and difference in thermal expansion coefficients.

Acknowledgements

The authors thank Ron Clissold for his help with the sample preparation and crack length measurement. One of the authors (N.C.) thanks the Volkswagenstiftung for supporting his sabbatical stay in the CSIRO, Australia. The authors also wish to thank a reviewer for the constructive comments on the manuscript.

References

1. Aksay, A. I., Dabbs, D. M. and Sarikaya, M., Mullite for structure, electronic, and optical applications. *J. Am. Ceram. Soc.*, 1991, **74**, 2343–2358.
2. Moya, J. S., Reaction sintered mullite–zirconia and mullite–zirconia–sic ceramics. In *Ceramic Transactions, Vol. 6, Mullite and Mullite Matrix Composites*, ed. S. Somiya, R. F. Davis and J. A. Pask. American Ceramic Society, Westerville, OH, 1987, pp. 495–507.
3. Claussen, N., Janssen, R. and Holz, D., Reaction bonding of aluminum oxide (RBAO)—science and technology. *J. Ceram. Soc. Japan*, 1995, **103**(8), 749–758.
4. Scheppokat, S., Claussen, N. and Hannink, R., RBAO composites containing TiN and TiN/TiC. *J. Euro. Ceram. Soc.*, 1996, **16**(9), 919–927.
5. Holz, D., Wu, S., Scheppokat, S. and Claussen, N., Effect of processing parameters on phase and microstructure evolution in RBAO ceramics. *J. Am. Ceram. Soc.*, 1994, **77**(10), 2509–2517.
6. Wu, S. and Claussen, N., Fabrication and properties of low-shrinkage reaction-bonded mullite. *J. Am. Ceram. Soc.*, 1991, **74**(10), 2460–2463.
7. Wu, S. and Claussen, N., Reaction bonding and mechanical properties of mullite/silicon carbide composites. *J. Am. Ceram. Soc.*, 1994, **77**(11), 2898–2904.
8. Matsumoto, R. L. K., Evaluation of fracture toughness determination methods as applied to ceria-stabilised tetragonal zirconia polycrystal. *J. Am. Ceram. Soc.*, 1987, **70**(12), c–366-c-368.
9. Anstis, G. R., Chantikul, P., Lawn, B. R. and Marshall, D. B., A critical evaluation of indentation techniques for measuring fracture toughness—direct crack measurements. *J. Am. Ceram. Soc.*, 1981, **64**, 533.
10. Bell, T. J., Bendeli, A., Field, J. S., Swain, M. V. and Thwaite, E. G., The determination of surface plastic and elastic properties by ultra micro indentation. *Metrologia*, 1991, **28**, 463–469.
11. Loubet, J. L., George, J. M., and Meille, G., Vickers indentation curves of elastoplastic materials. In *Microindentation Techniques in Materials Science and Engineering*, ed. P. J. Blau and B. R. Lawn. American Society for Testing and Materials, Philadelphia, PA, 1986, pp. 72–89.
12. Jacobson, N. S., Lee, K. N. and Fox, D. S., Reactions of silicon carbide and silicon (IV) oxide at elevated temperatures. *J. Am. Ceram. Soc.*, 1992, **75**(6), 1603–1611.
13. Schiroky, G. H., Oxidation behaviour of chemically vapour-deposited silicon carbide. *Advanced Ceramic Materials*, 1987, **2**(2), 137–141.
14. Dukino, R. D. and Swain, M. V., Comparative measurement of indentation fracture toughness with berkovich and vickers indenter. *J. Am. Ceram. Soc.*, 1992, **75**(12), 3299–3304.